Int. J. Electrochem. Sci., 9 **(2014)** 7309 - 7324

International Journal of
ELECTROCHEMICAL
SCIENCE
www.electrochemsci.org

Investigation of a Pharmaceutically Active Compound Omeprazole as Inhibitor for Corrosion of Mild Steel in H_2SO_4 Solution

Xiaofang Luo, Shengtao Zhang[*], *Lei Guo*

School of Chemistry and Chemical Engineering, Chongqing University, Chongqing 400044, PR China
[*]E-mail: stzhcq@163.com

Received: 1 August 2014 / *Accepted:* 15 September 2014 / *Published:* 29 September 2014

Inhibition performance of omeprazole for mild steel in 0.1M H_2SO_4 solution has been investigated through different approaches including potentiodynamic polarization, electrochemical impedance spectroscopy (EIS), weight loss, scanning electron microscope (SEM) experiments and theoretical calculations. The experimental results reveal that omeprazole is an effective inhibitor with a maximum achievable inhibition efficiency of 98.5%, and the adsorption of omeprazole on the mild steel surface is found to obey the Langmuir adsorption isotherm. Polarization curves illustrate that omeprazole acts as a mixed-type inhibitor, and EIS demonstrates that an adsorption film of the inhibitor is formed on mild steel surface. Moreover, quantum chemical calculations and the molecular dynamics (MD) simulation are also performed to gain the further insight of the inhibition mechanism of omeprazole on steel corrosion, which show that the possible adsorption centers of the omeprazole molecule are benzene ring, benzimidazole ring, sulphinyl and the nitrogen atom of the hexaheterocyclic.

Keywords: mild steel, EIS, polarization, weight loss test, acid inhibition, omeprazole

1. INTRODUCTION

The corrosion of steel is a fundamental academic and industrial concern that has received a considerable amount of attention. Acid solutions are extensively used in many industrial processes such as acid pickling, industrial acid cleaning, oil-well acidizing, which leads to corrosive attack. In the past few years, numerous inhibitors have been investigated to study their inhibitive effect, as well as the relationship between inhibitor molecular structure and corresponding inhibition efficiency [1-4]. The majority of the well-known inhibitors are organic compounds containing heteroatoms, such as oxygen, nitrogen or sulphur, and multiple bonds, which allow an adsorption on the metal surface [5-7]. As we know, a great amount of commercial inhibitors are toxic, hence the researchers are paying more

attention on development of environment-friendly inhibitors in recent years. For this aim of the present investigation, many pharmaceutically active compounds [8-10] and many plants extract [11-13] have been estimated as effective corrosion inhibitors for different metals and alloys in various aggressive environments. However, the corrosion inhibition performance of omeprazole on mild steel in sulfuric acid medium was not reported so far to the best of our knowledge.

Omeprazole (6-methoxy-2-[(R)-(4-methoxy-3,5-dimethylpyridin-2-yl)methylsulfinyl]-1*H*-benzoimidazole) is an anti-ulcer drug and used for short term treatment for erosion. As shown in Figure 1, the molecular structure of omeprazole contains a large number of donating atoms (N, O, S atoms) which provides a theoretical consideration for its inhibitive action study. The choice of omeprazole as corrosion inhibitor is based on its low toxicity, relatively cheap and high solubility in acidic media. Quantum chemical calculations have been proved to be a very powerful tool for studying the inhibition mechanism [14-16]. Recently, the molecular dynamic method, often used to study the interaction of phase interfaces, has been applied to research the interaction between inhibitors and metal surface [17-20].

Therefore in the present work omeprazole is investigated as the inhibitor for mild steel Q235 corrosion in 0.1 M H_2SO_4 at 298 K. The inhibition effect of omeprazole was evaluated by means of weight loss measurement, potentiodynamic polarization, and electrochemical impedance spectroscopy. Quantum chemical calculations were further employed to explain the inhibition efficiency of omeprazole and the fundamental mechanism of omeprazole adsorption on iron surface was studied by molecular dynamics method.

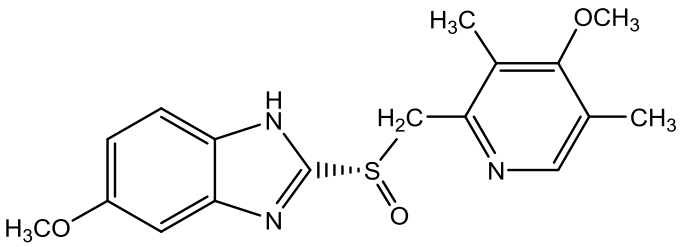

Figure 1. Molecular structure of omeprazole.

2. EXPERIMENTAL PART

2.1. Materials and sample preparation

The working electrode used in this experiment is mild steel Q235 (chemical composition: 0.17% C, 0.47% Mn, 0.26% Si, 0.017% S, 0.0048% P and the remainder iron), which was mechanically cut into 3.0 cm × 2.0 cm × 1.0 cm dimensions for weight loss measurement, and 1.0 cm × 1.0 cm × 1.0 cm dimensions for SEM measurement. For electrochemical tests, the specimens were imbedded in epoxy resin with a surface area of 1.00 cm^2 exposed to the corrosive medium. The surfaces of all the specimens were abraded with SiC paper of 400, 800, 1000, and 1200 grades, washed thoroughly with distill water, degreased ultrasonically in acetone and finally dried.

The test solutions were prepared using analytical grade 97% H_2SO_4 and distilled water. The test inhibitor omeprazole obtained from Aladdin® was added in acid solution range from 5×10^{-5} to 1×10^{-3} M, and the solution without the presence of omeprazole is taken as blank for comparison.

2.2. Electrochemical measurements

Polarization curves and electrochemical impedance spectroscopy are measured through CHI604D electrochemical workstation (Shanghai Chenhua CO, LTD) in a three electrode glass cell at 298 K. Before starting the experiments, a time interval of about 45 min is given for the system to reach a steady state and the open circuit potential is noted. The polarization curves are conducted from cathodic potential of −250 mV to an anodic potential of +250 mV at a scan rate of 2 mV s^{-1}. The EIS measurements is carried out over a frequency range extended from 10^{-2} Hz to 105 Hz with amplitude of 5 mV peak-to-peak. Nyquist plots are obtained from the results of these experiments after 45 min of immersion. The EIS parameters are analyzed by fitting the experimental results to an appropriate equivalent circuit using ZSimpWin software. All the electrochemical tests are repeated at least three times under the same situation to confirm the accuracy of data obtained.

2.3. Weight loss experiments

The weight loss measurements are carried out in a 250 mL glass beaker placed in a water bath with thermostat control. Mild steel specimens were accurately weighted and then immersed in 0.1 M H_2SO_4 solutions for 24 h in the absence and presence of various concentrations of omeprazole at 298 K. After the immersion, the specimens are taken out washed, dried and weighed accurately. Duplicate experiments are performed on the same condition and the mean value of the weight loss is reported.

2.4. SEM analysis

After immersion in 0.1 M H_2SO_4 solution in the absence and presence of 1×10^{-3} M omeprazole for 24 h, the surface morphologies of mild steel specimens are performed on a scanning electronic microscope (TESCAN VEGA II) at 25 kV.

2.5. Theory and computation details

DFT calculations for the omeprazole molecule are accomplished by means of the Gaussian 03 program to analyze the structural and electronic parameters; the structures are fully optimized, and vibrational analyses are carried out to verify that the optimized geometries corresponded to minimum global energy. The popular Becke's three-parameter hybrid functional (B3LYP) [21] method in combination with the 6-31G basis set has been chosen.

The forcite molecular dynamics module in Material Studio 6.0 software is employed to conduct the molecular dynamics simulations of the interaction between the omeprazole dissolved in

H_2O and the Fe(110) surface in a simulation box (27.3 Å × 24.8 Å × 39.2 Å) with periodic boundary conditions. Omeprazole molecule is energy optimized, Fe(110) surface and water layers was constructed using the amorphous cell module. COMPASS (Condensed Phase Optimized Molecular Potentials for Atomistic Simulation Studies) was used to optimize the structures of all components of the system of interest represents a technology break-through in force field method [22]. It is the first ab initio forcefield that enables accurate and simultaneous prediction of chemical properties (structural, conformational, vibrational, *etc.*) and condensed-phase properties (equation of state, cohesive energies, *etc.*) for a broad range of chemical systems. It is also the first high quality forcefield to consolidate parameters of organic and inorganic materials. Temperature was fixed at 298 K, with NVT ensemble, with a time step of 1 fs and simulation time of 1 ns. The interaction energy $E_{\text{Fe-inhibitor}}$ of Fe surface with the omeprazole is calculated according to the following equation:

$$E_{\text{Fe-inhibitor}} = E_{\text{complex}} - \left(E_{\text{Fe}} + E_{\text{inh}}\right) \quad (1)$$

where E_{complex} is the total energy of the Fe crystal together with the adsorbed inhibitor molecule, E_{Fe} and E_{inh} is the total energy of the iron crystal and free inhibitor molecule, respectively. The binding energy is the negative value of the interaction energy $E_{\text{binding}} = -E_{\text{Fe-inhibitor}}$.

3. RESULTS AND DISCUSSION

3.1. Electrochemical impedance spectroscopy experiments

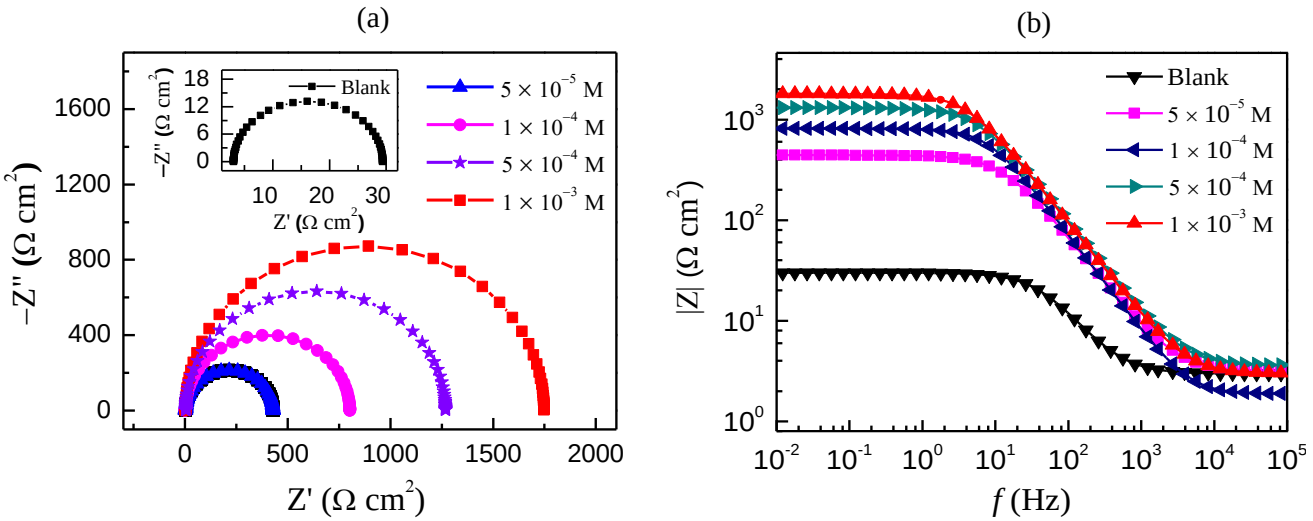

Figure 2. Nyquist (a), and Bode (b) plots for mild steel in 0.1 M H_2SO_4 solution with different concentrations of omeprazole at 298 K.

The impedance spectra for mild steel in 0.1 M H_2SO_4 solution with different concentrations of omeprazole are presented as Nyquist and Bode plots in Figure 2. It is apparent that the impedance response of mild steel has significantly changed after the addition of omeprazole in the corrosive solutions. As seen from Figure 2a, the Nyquist plots show that a single semicircle and the diameter of semicircle increases with increasing inhibitor concentration, indicating that the corrosion process on

steel is mainly dominated by the charge transfer process [12]. We can also find that these Nyquist plots appear as depressed semicircles but not the perfect semicircles, this is probably attributed to the inhomogeneity of the metal surface resulting from the roughness of the electrode surface or interfacial effect. Moreover, the diameter of semicircle increases substantially and the impedance values over the whole frequency range increase with increasing omeprazole concentration as shown in Figure 2b, demonstrating that the corrosion resistance of mild steel has been enhanced significantly.

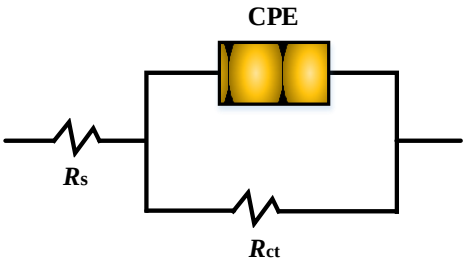

Figure 3. Electrical equivalent circuit used to fit the EIS experiment data.

The electrical equivalent circuit model is shown in Figure 3, which is used to analyse the obtained data. This equivalent circuit consists of a constant phase element (CPE), in parallel with a resistor (R_{ct}). The CPE is often used to substitute the double layer capacitance (C_{dl}) to give a more accurate fit of the experimental impedance data. In this designed circuit, the R_s reflects the resistance of the solution between the working electrode and saturated calomel electrode, R_{ct} represents the charge-transfer resistance, CPE is constituted of component Y_0 and a coefficient n. The impedance of the CPE is given by [23]:

$$Z_{CPE} = \frac{1}{Y_0(j\omega)^n} \qquad (2)$$

where Y_0 is the CPE constant, j is the imaginary unit, ω is the angular frequency, and n is the deviation parameter which is often related to the surface morphology. Different values of n ($-1 \le n \le 1$) give the CPE different electrical component presentation. The impedance parameters derived from these plots are given in Table 1. The double layer capacitance (C_{dl}) [24] and inhibition efficiency (η_R) can be calculated according to the Eq. (3) and (4), respectively:

$$C_{dl} = (Y_0 R_{ct}^{1-n})^{1/n} \qquad (3)$$

$$\eta_R = \frac{R_{ct} - R_{ct,0}}{R_{ct}} \times 100 \qquad (4)$$

where R_{ct} and $R_{ct,\,0}$ are the charge transfer resistance in the presence and absence of omeprazole, respectively.

As seen from the Table 1, the R_{ct} value increase with increasing omeprazole concentration and however, C_{dl} value decreases much in the presence of omeprazole. This situation is a result of the adsorption of inhibitor molecules at the metal/solution interface. The varying concentration of omeprazole in acid solution from 5×10^{-5} to 1×10^{-3} M leads to the change of the inhibition efficiencies from 93.8% to 98.5%, indicating that the omeprazole is a high effective inhibitor for steel

corrosion in H_2SO_4 solution. As for the C_{dl}, in Helmholtz model, it can be expressed as the following relation [25]:

$$C_{dl} = \frac{\varepsilon^0 \varepsilon}{d} S \qquad (5)$$

where ε^0 is the vacuum permittivity, ε is the local dielectric constant of the medium, d is the thickness of interfacial film and S is the surface area of the working electrode. According to this formula, it is noticeable that C_{dl} decreases, while the adsorption coverage increased with the S and the ε value decreases. Thus it could be assumed that the decrease of C_{dl} values is caused by the gradual replacement of water molecules by adsorption of the inhibitor molecules which have larger size and smaller dielectric constant compared to the water molecules. Also the values of n decrease with the increasing of omeprazole concentration illustrates that the adsorption effect of inhibitor gives rise to the inhomogeneity of the steel surface.

Table 1. Electrochemical impedance parameters for mild steel in 0.1 M H_2SO_4 with different concentrations of omeprazole at 298 K.

C (M)	R_s (Ω cm^2)	CPE		R_{ct} (Ω cm^2)	C_{dl} (μF cm^{-2})	η_R
		Y_0 ($\times 10^{-5}$ $S s^n$ cm^{-2})	n			
Blank	2.97	25.70	0.9027	26.3	51.88	/
5×10^{-5}	3.16	4.329	0.9035	425.1	9.66	93.8
1×10^{-4}	1.87	2.884	0.9090	800.5	6.40	96.7
5×10^{-4}	3.59	2.867	0.9107	1265.0	5.48	97.9
1×10^{-3}	2.99	2.735	0.9242	1745.0	4.02	98.5

3.2. Polarization measurements

Potentiodynamic polarization measurements are carried out immediately after the EIS experiments. Figure 4 shows the polarization curves for mild steel in 0.1 M H_2SO_4 in the absence and presence of varying concentrations of omeprazole at 298 K. All the electrochemical parameters such as the corrosion potential (E_{corr}), corrosion current density (i_{corr}), Tafel slopes β_a (β_c) are listed in Table 2. The inhibition efficiency (η_p) is evaluated from the calculated i_{corr} values according to the equation:

$$\eta_P = \frac{i^0_{corr} - i_{corr}}{i^0_{corr}} \times 100 \qquad (6)$$

where i^0_{corr} and i_{corr} are the corrosion current densities in the absence and the presence of omeprazole, respectively.

According to literatures reported previously [24-26], the reaction process of mild steel in H_2SO_4 solution can be described as follows:

$$Fe \longrightarrow Fe^{2+} + 2e^-$$

$$2H^+ + 2e^- \longrightarrow H_2$$

For the dissolution of mild steel in acid solutions, at equilibrium the total anodic rate is equal to the total cathodic rate [27]:

$$\left|i_H^{\rightarrow}\right| + \left|i_{Fe}^{\rightarrow}\right| = i_H^{\leftarrow} + i_{Fe}^{\leftarrow}$$

where the forward arrow refers to the cathodic direction.

The electrode potential of the steady-state freely corroding condition given by the above equation is called the corrosion potential E_{corr} [17], which lies between the equilibrium potentials of the two individual half-cell reactions. At E_{corr}, the following equation gives:

$$i_{corr} = i_{Fe}^{\leftarrow} - \left|i_{Fe}^{\rightarrow}\right| = \left|i_H^{\rightarrow}\right| - i_H^{\leftarrow}$$

Thus, either hydrogen evolution or iron dissolution net rate can be measured at E_{corr}, which gives i_{corr} at the freely corroding condition. Moreover, for such a system the Tafel equation is modified to give:

$$E = a + b \log i$$

where a and b are constants. In the Tafel equation, when $E = E_{corr}$, then $i = i_{corr}$. This is the basis for the Tafel extrapolation.

As shown in Figure 4a, Tafel lines are shifted to more negative and more positive potentials with respect to the blank curve by increasing the concentration of the inhibitors. From the cathodic part of polarization, the cathodic curves in inhibited solutions are almost in parallel with the blank experimental one, suggesting that the hydrogen evolution is activation-controlled and the reduction mechanism is not affected by the presence of the inhibitor. These results demonstrate that omeprazole exhibits both cathodic and anodic inhibition effects and acts as a mixed-type inhibitor. From the anodic region of polarization curves, it can be observed that a remarkable inhibiting effect in the inhibitor-containing solutions exists at the initial overpotential stage, this is probably attributed to the protective film formed on the steel surface to limit the contact between H^+ ions and iron. In addition, when the potential is higher than −0.3 V, it seems omeprazole exhibits no effect on the anodic polarization curves.

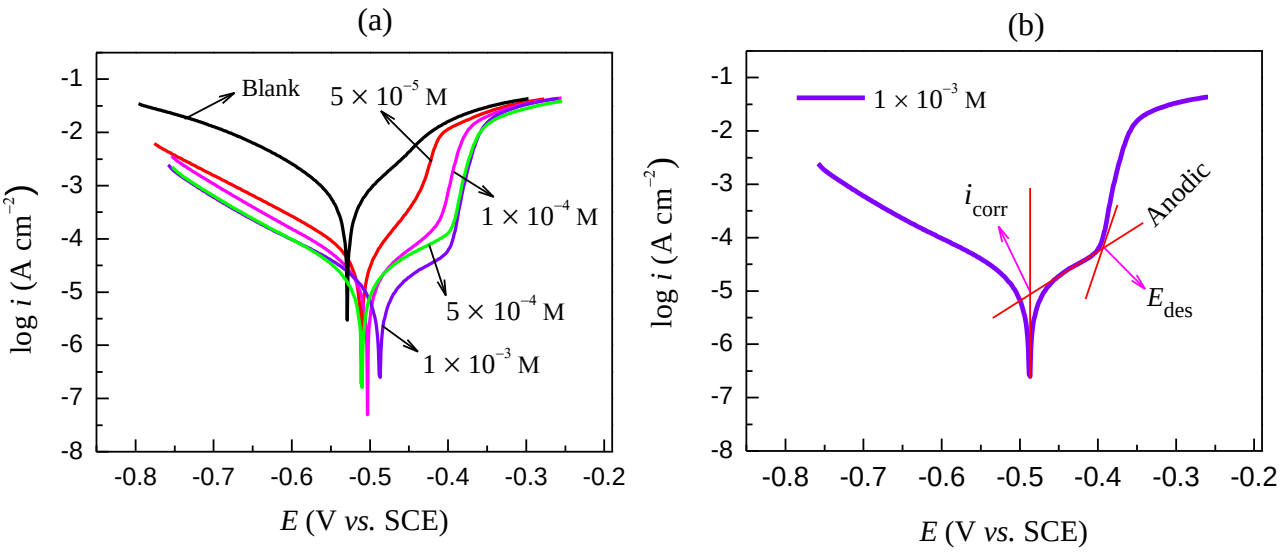

Figure 4. (a) Potentiodynamic polarization curves for mild steel in 0.1 M H_2SO_4 containing different concentrations of omeprazole; (b) Tafel extrapolation of the anodic polarization curve.

We can see clearly that both the anodic and cathodic branches of the polarization curve exhibit a typical Tafel behavior. The corrosion rate can be determined by Tafel extrapolation method [9,25], and both branches can be extrapolated back to the corrosion potential E_{corr} to give the corrosion rate i_{corr}. This is because the net rate of iron dissolution is equal to the net rate of hydrogen evolution at the open-circuit corrosion potential. As shown in Figure 4b, the Tafel line of the anodic polarization curve is extended to the electrode potential below the corrosion potential, and then a line is made vertical to the X-axis at the corrosion potential. The electrochemical parameters can be obtained from the intersection points [17], which are listed in Table 2.

Similarly in Figure 4b, as the polarization potential moves a certain value (about −100 mV), a plat form in vertical can be seen on the anodic curves especially at relatively high inhibitor concentration. This can be explained by desorption of the omeprazole molecules from the electrode surface due to the significant dissolution of steel. In this case the desorption rate of omeprazole is higher than its adsorption rate, so the corrosion current increased more significantly with rising potential. Between the extended Tafel line of the polarization curve and the flat region, there is a potential of the intersection point which can be described as desorption potential. According to the Table 2, it's obviously find that the desorption potentials (E_{des}) move to more positive values with increasing inhibitor concentration, in other words, the adsorbed inhibitor molecules get more stable on the surface.

Inspection of Table 2 reveals that the corrosion current (i_{corr}) decreased prominently and inhibition efficiency increased with increased inhibitor concentration. Also the β_a, β_c values changed slightly with addition of omeprazole, indicating that omeprazole functions via blocking the reaction sites on the metal surface without changing the anodic and cathodic reaction mechanisms. If the largest displacement of E_{corr} value surpasses ±85 mV, the inhibitor can be cathodic or anodic type inhibitor. According to the E_{corr} values listed in Table 2, the largest E_{corr} shift is 26 mV, which indicates that the omeprazole can be classified as a mixed-type inhibitor. At the concentration of 1×10^{-3} M omeprazole, the highest inhibition efficiency reaches 97.8%. It is enough to say that omeprazole exhibits a superb inhibition property for mild steel corrosion in 0.1 M H_2SO_4 at 298 K.

Table 2. The potentiodynamic polarization parameters for mild steel in 0.1 M H_2SO_4 solution without and with the presence of different concentration of omeprazole at 298 K.

C (M)	E_{corr} (mV)	i_{corr} (μA cm^{-2})	β_c (mV dec^{-1})	β_a (mV dec^{-1})	E_{des} (mV)	η_p
Blank	–529	504.8	10.639	12.934	/	/
5×10^{-5}	–511	30.25	15.615	20.837	–428	94.01
1×10^{-4}	–503	20.74	10.595	11.497	–396	95.89
5×10^{-4}	–510	15.09	7.911	9.735	–385	97.01
1×10^{-3}	–503	11.13	8.296	12.945	–372	97.80

3.3. Weight loss experiments

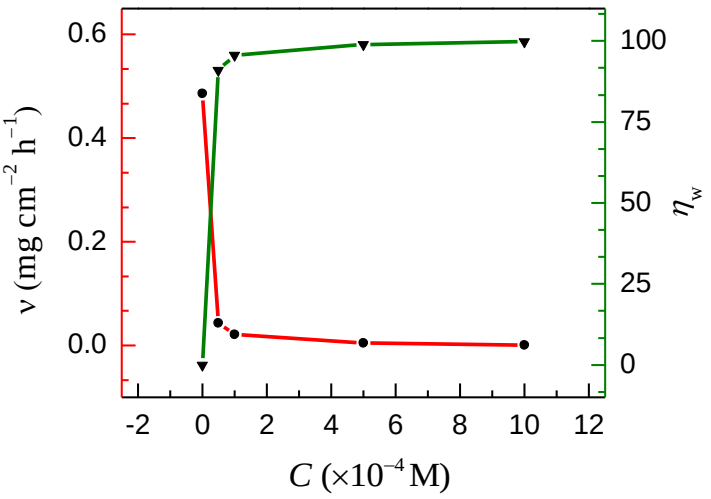

Figure 5. Corrosion rates and inhibition efficiencies for mild steel in 0.1 M H_2SO_4 with different concentrations of omeprazole at 298 K.

Figure 5 shows the corrosion rate (v, mg cm^{-2} h^{-1}) and the inhibition efficiency (η_w) at different concentrations of omeprazole after 24 h immersion in 0.1 M H_2SO_4 at 298 K. They are calculated from the following equations:

$$v = \frac{\Delta W}{St} \qquad (7)$$

where ΔW is the average weight loss (mg) of three parallel steel specimens, S is the total area of specimens (cm^2), and t is the immersion time (h).

$$\eta_w = \frac{v_0 - v}{v_0} \times 100 \qquad (8)$$

where v_0 and v are the corrosion rate of steel in the 0.1 M H_2SO_4 solution without and with the addition of omeprazole, respectively.

It can be seen from Figure 5, corrosion rate decreases significantly after the omeprazole is added into the corrosive medium and the inhibition efficiency increases with increasing the concentration of omeprazole. This result is ascribed to the fact that the adsorption amount and coverage of inhibitor on mild steel surface increases with inhibitor concentration. As the concentration reached to 1×10^{-3} M, η_w of omeprazole gained a high value of 99.8% at 298 K, which suggests that omeprazole is an effective corrosion inhibitor in acid solution. The inhibition efficiencies obtained from weight lost measurements are in accordance with those in the EIS and polarization experiments.

3.4. Adsorption isotherm

The adsorption of organic adsorbate on a metal surface is regarded as a substitutional adsorption process between the inhibitor molecule in the aqueous solution ($Inh_{(sol)}$), and water

molecules adsorbed on the metallic surface ($H_2O_{(ads)}$). The adsorption behavior can be depicted as the following substitution process [26]:

$$Inh_{(sol)} + xH_2O_{(ads)} \rightarrow Inh_{(ads)} + H_2O_{(sol)} \quad (9)$$

where $Inh_{(sol)}$ and $Inh_{(ads)}$ refer to the inhibitor specie dissolved in aqueous solution and adsorbed on metal surface, respectively, x is the number of water molecules substituted by inhibitor adsorbate.

The adsorption isotherms to fit the experimental data generally considered are [27]:

- Frumkin isotherm $\frac{\theta}{1-\theta}\exp(-2f\theta) = K_{ads}C$
- Freundluich isotherm $\theta = K_{ads}C$
- Temkin isotherm $\exp(f\theta) = K_{ads}C$
- Langmuir isotherm $\frac{\theta}{1-\theta} = K_{ads}C$

where C is the inhibitor concentration, K_{ads} is the adsorption equilibrium constant, and f is the factor of energetic inhomogeneity. θ is the surface coverage and can be evaluated as η_w in accordance with Figure 5. But ultimately, the results show that the Langmuir adsorption isotherm is found to be the best description of the adsorption behaviors of omeprazole. Langmuir adsorption also can be described as following equation:

$$\frac{C}{\theta} = \frac{1}{K_{ads}} + C \quad (10)$$

As shown in Figure 6, the plots of C *vs* C/θ yield straight line with nearly unit slope showing that the adsorption of omeprazole on the mild steel surface follows Langmuir adsorption isotherm. The linear regression coefficient is almost equal to 1, indicating that the adsorbed molecules occupy only one site and there is no interaction occurring between the adsorbed inhibitor molecules.

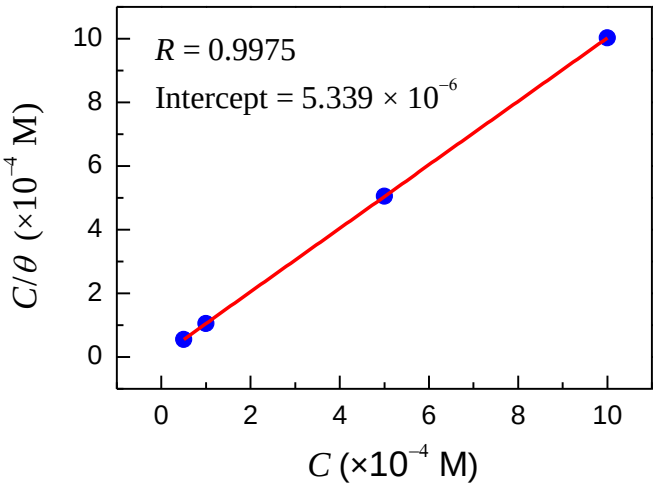

Figure 6. Langmuir adsorption isotherm of omeprazole in 0.1 M H_2SO_4 at 298 K.

The free energy of adsorption (ΔG_{ads}) can be calculated from Eq. (11) [28]:

$$\Delta G_{ads} = -RT\ln(55.5K_{ads}) \quad (11)$$

where R is the universal gas constant, T is the thermodynamic temperature, the value of 55.5 is the molar concentration of water in the solution expressed in mol L^{-1}, the value of $1/K_{ads}$ is 5.339×10^{-6} can be determined from the intercepts of the straight lines on the C/θ-axis. Then according to Eq. (11), the standard free energy of adsorption can be calculated, and the value of $\Delta G_{ads} = -40.32$ kJ mol^{-1}. The negative values of ΔG_{ads} indicate that the adsorption of omeprazole is a spontaneous process.

The adsorption of inhibitor compounds can be described by two main types of interaction: physisorption and chemisorption. Generally, if the value of ΔG_{ads} is around 20 kJ mol^{-1} or lower, the type of adsorption can be seen as physisorption, and the inhibitive effect is duo to electrostatic interactions between the charged molecules and the charged metal. And when the value of ΔG_{ads} is around 40 kJ mol^{-1} or higher, the adsorption can be regarded as chemisorption and the inhibitive effect is coming from the result of sharing or transfer of electrons from inhibitor to the metal surface to form a covalent bond. The absolute values of ΔG_{ads} is higher than 40 kJ mol^{-1}, implying that the adsorption mechanism of omeprazole on the mild steel surface is the chemisorption and it links to the surface by covalent forces.

3.5. SEM analyses

The surface micrographs of mild steel specimens before immersion in 0.1 M H_2SO_4 show a freshly polished steel surface Figure 7a). SEM photographs obtained from mild steel surface after specimens immersion in 0.1 M H_2SO_4 in the absence and presence of 1×10^{-3} M omeprazole are shown in Figure 7b and 7c, respectively. The rough and severely damaged surface is presented in the Figure 6b, suggesting an immense corrosion effect on steel by acid solution without containing any inhibitor. In contrast, in the presence of omeprazole (Figure 7c), the surface is well protected and much less damaged. These images reveal that the omeprazole is a high effective inhibitor for mild steel corrosion in acid solution.

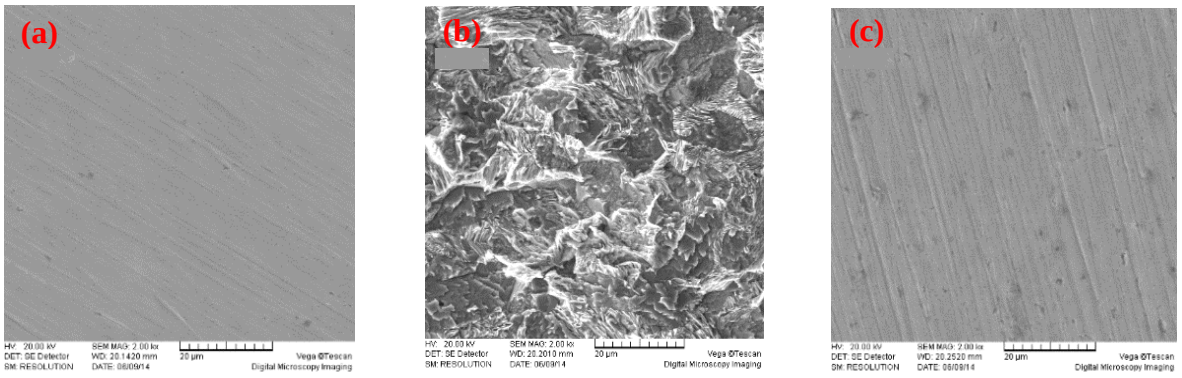

Figure 7. SEM micrographs of freshly polished specimen (a) and the specimens immersed in 0.1 M H_2SO_4 solution for 24 h at 298 K without inhibitor (b), with 1×10^{-3} M omeprazole (c).

3.6. Theoretical study

3.6.1. Quantum chemical calculations

Frontier orbital theory is useful in predicting adsorption centers of the inhibitor molecules responsible for the interaction with surface metal atoms [29]. The optimized molecule structure, the highest occupied molecule orbitals (HOMO), the lowest unoccupied molecule orbital (LUMO), and the electrostatic potential (ESP) distribution of omeprazole molecule using DFT functional (B3LYP/6-31G) are shown in Figure 8. The energies of the HOMO and LUMO of the molecule and energy gap ($\Delta E = E_{LUMO} - E_{HOMO}$) are found to be −5.84 eV, −1.44 eV and 4.39 eV, respectively. It can be observed that the HOMO is mainly distributed in the benzimidazole ring, sulphinyl and the N/O atoms. The HOMO of omeprazole have a considerable excess of negative charge. Hence, omeprazole can be adsorbed on the iron surface by donating the unshared pair of electrons from the N, S, and O atoms to the vacant *d* orbitals of iron.

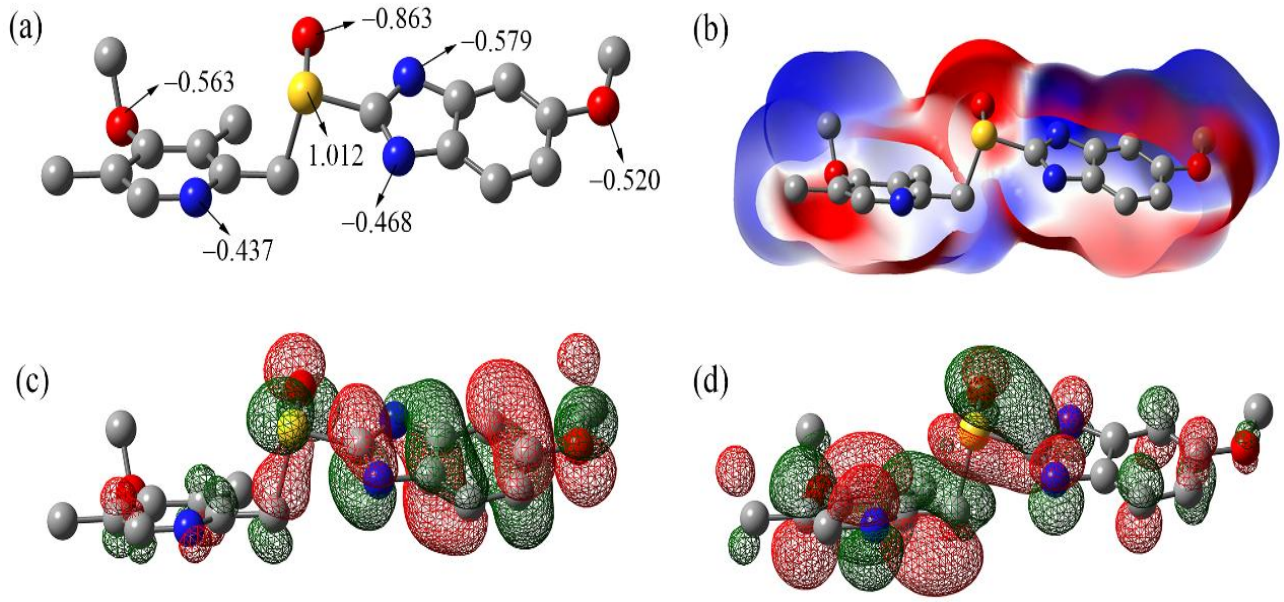

Figure 8. Quantum chemistry calculations results of omeprazole molecule: (a) optimized structure with NPA charge of heteroatoms, (b) population of ESP, (c) population of HOMO, (d) population of LUMO.

According to previous reports [30], the number of transferred electrons (ΔN) showed inhibition effect resulted from electron donation. It was calculated according to Eq. (12)

$$\Delta N = \frac{\chi_{Fe} - \chi_{inh}}{2(\eta_{Fe} + \eta_{inh})} \quad (12)$$

where χ_{Fe} and χ_{inh} denote the absolute electronegativity of iron and the inhibitor molecule, respectively; η_{Fe} and η_{inh} denote the absolute hardness of iron and the inhibitor molecule, respectively. These quantities are related to electron affinity (A) and ionization potential (I)

$$\chi = \frac{I + A}{2} \quad (13)$$

$$\eta = \frac{I - A}{2} \quad (14)$$

I and A are related in turn to E_{HOMO} and E_{LUMO}

$$I = -E_{HOMO} \quad (15)$$

$$A = -E_{LUMO} \quad (16)$$

The theoretical values of χ_{Fe} and η_{Fe} are 7 eV mol^{-1} and 0 eV mol^{-1}, respectively. The calculated fraction of electrons transferred from omeprazole molecule to iron is 0.763. According to Lukovits [31], if $\Delta N < 3.6$, the inhibition efficiency increased with increasing electron-donating ability at the metal surface. In this study, the value of ΔN for omeprazole was less than 3.6. This shows that the increase in inhibition efficiency was due solely to the electron-donating ability of omeprazole. The omeprazole was bound to the mild steel surface, and thus formed inhibition adsorption layer against corrosion.

3.6.2. Molecular dynamic simulation

The molecular dynamic simulations are performed to study the adsorption behavior of omeprazole on the Fe(110) surface. Whether the model system has reached equilibrium or not is ascertained by the equilibrium criterions of temperature and energy simultaneously, *i.e.*, the fluctuations of temperature and energy should be confined to 5−10% [32]. According to the temperature and energy curves from MD simulations at 298 K (Figure 9), the temperature fluctuates in a range of (298 ± 15) K and the fluctuation of energy is less than 0.5%, indicating that the system has reached an equilibrium state.

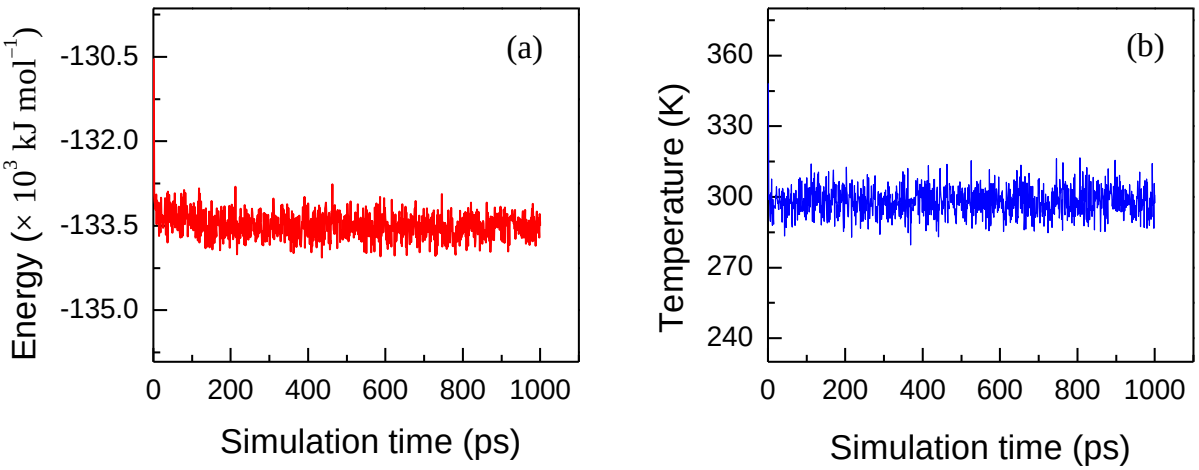

Figure 9. Energy fluctuant (a) and temperature equilibrium curves (b) of omeprazole molecule on Fe(110) surface.

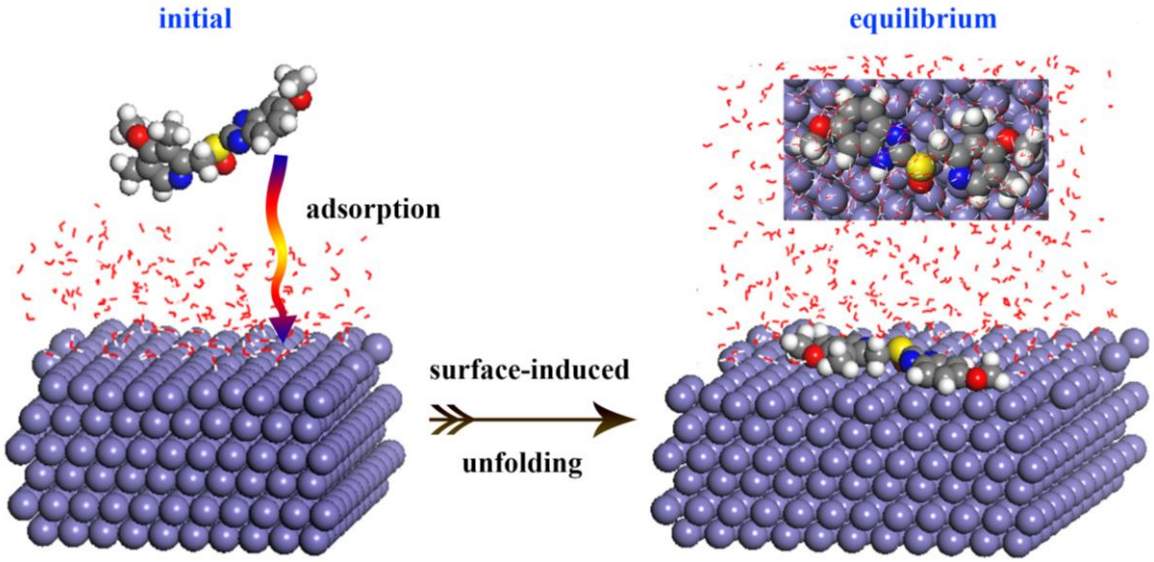

Figure 10. Omeprazole adsorbed on Fe(110) surface in water solution.

Figure 10 shows the initial and equilibrium configurations of omeprazole in water solution. It can be easily seen from Figure 10 that omeprazole molecule gradually moves to the iron surface, and when the adsorption process reaches a balance, all the atoms are almost in the same plane, and the omeprazole molecule is nearly parallel to the target surface. The omeprazole molecule is subjected to a substantial degree of reconstruction. The deformation degree of absorbed molecule was evaluated by deformation energy (E_{deform}):

$$E_{deform} = E_{inh\text{-}bind} - E_{inh} \quad (17)$$

where $E_{inh\text{-}bind}$ and E_{inh} are single point energies of inhibitor molecule in adsorbed and free states, respectively. The result we get is E_{deform} = 202.5 kJ mol^{-1}. This made a significant contribution to improve the inhibition efficiency. We can draw a conclusion that the omeprazole can be absorbed on Fe(110) surface through the benzimidazole/pyridine rings and the S/O/N atoms. A number of lone pairs electrons on heteroatoms as well as π-electron clouds on the aromatic ring contribute a great deal to the adsorption process. This planar adsorption configuration increases the contact area and prevents the water molecule from penetrating into the iron surface. The calculated value of binding energy for the adsorption of omeprazole on iron surface in the presence of water molecules was 948.5 kJ mol^{-1}, implies that the omeprazole molecules adsorbed easily on the mild steel surface.

4. CONCLUSIONS

EIS experiments results reveal that the charge transfer resistances of the mild steel electrode increases greatly while the double layer capacitance decreases with increasing the inhibitor concentration, implying that omeprazole inhibits through adsorption mechanism. Polarization curves indicate that omeprazole acts as a mix-type inhibitor, which show that omeprazole inhibits both the anodic and cathodic processes of the corrosion of mild steel in 0.1 M H_2SO_4 solution. SEM shows that

mild steel corrosion can be inhibited effectively due to the adsorption of omeprazole on the steel surface. Thermodynamic calculation indicates that the adsorption of omeprazole follows well the Langmuir isotherm and the chemisorption is involved in the interaction between inhibitors and the mild steel surface. The quantum chemical calculations and molecular dynamics simulation illustrate that the omeprazole molecule can be adsorbed on mild steel surface through the benzene ring, benzimidazole ring, sulphinyl and the heteroatoms. All measurements results obtained demonstrate that omeprazole has excellent inhibition properties for mild steel in sulfuric acid solution.

ACKNOWLEDGEMENTS
This research is sponsored by the National Natural Science Foundation of China (21376282).

References

1. M.M. Antonijevic, M.B. Petrovic, *Int. J. Electrochem. Sci.*, 3 (2008) 1.
2. Y.G. Avdeev, Y.I. Kuznetsov, *Russ. Chem. Rev.*, 81 (2012) 1133.
3. B.E.A. Rani, B.B.J. Basu, *Int. J. Corros.*, 2012 (2012) 1.
4. E.E. Oguzie, Y. Li, S.G. Wang, F. Wang, *RSC Adv.*, 1 (2011) 866.
5. N.S. Patel, S. Jauhari, G.N. Mehta, *Chem. Pap.*, 64 (2010) 51.
6. A. Zarrouk, B. Hammouti, A. Dafali, F. Bentiss, *Ind. Eng, Chem, Res.*, 52 (2013) 2560.
7. K.F. Khaled, *Electrochim. Acta*, 53 (2008) 3484.
8. G. Gece, *Corros. Sci.*, 53 (2011) 3873.
9. S.K. Shukla, M.A. Quraishi, *Mater. Chem. Phys.*, 120 (2010) 142.
10. I. Ahamad, R. Prasad, M.A. Quraishi, *Corros. Sci.*, 52 (2010) 3033.
11. O. Benali, C. Selles, R. Salghi, *Res. Chem. Intermed.*, 40 (2014) 259.
12. K. Krishnaveni, J. Ravichandran, A. Selvaraj, *Ionics*, 20 (2014) 115.
13. I.M. Mejeha, M.C. Nwandu, K.B. Okeoma, L.A. Nnanna, M.A. Chidiebere, F.C. Eze, E.E. Oguzie, *J. Mater. Sci.*, 47 (2011) 2559.
14. G. Gece, *Corros. Sci.*, 50 (2008) 2981.
15. M.S. Masoud, M.K. Awad, M.A. Shaker, M.M.T. El-Tahawy, *Corros. Sci.*, 52 (2010) 2387.
16. N.O. Obi-Egbedi, I.B. Obot, M.I. El-Khaiary, S.A. Umoren, E.E. Ebenso, *Int. J. Electrochem. Sci.*, 6 (2011) 5649.
17. E.E. Oguzie, M.A. Chidiebere, K.L. Oguzie, C.B. Adindu, H. Momoh-Yahaya, *Chem. Eng. Commun.*, 201 (2014) 790.
18. J.J. Fu, H.S. Zang, Y. Wang, S.N. Li, T. Chen, X.D. Liu, *Ind. Eng, Chem, Res.*, 51 (2012) 6377.
19. K.F. Khaled, M.A. Amin, *J. Appl. Electrochem.*, 39 (2009) 2553.
20. J. Li, X.L. Xu, K. Shi, Y. Zhou, X. Luo, Y. Wu, *Int. J. Electrochem. Sci.*, 7 (2012) 9580.
21. C.T. Lee, W.T. Yang, R.G. Parr, *Phys. Rev. B*, 37 (1988) 785.
22. H. Sun, *J. Phys. Chem. B*, 102 (1998) 7338.
23. J.B. Jorcin, M.E. Orazem, N. Pebere, B. Tribollet, *Electrochim. Acta*, 51 (2006) 1473.
24. P. Zoltowski, *J. Electroanal. Chem.*, 443 (1998) 149.
25. S.T. Zhang, Z.H. Tao, S.G. Liao, F.J. Wu, *Corros. Sci.*, 52 (2010) 3126.
26. D.K. Yadav, B. Maiti, M.A. Quraishi, *Corros. Sci.*, 52 (2010) 3586.
27. H. Demiral, I. Demiral, F. Tumsek, B. Karabacakoglu, *Chem. Eng. J.*, 144 (2008) 188.
28. E.E.F. El-Sherbini, S.M.A. Wahaab, M. Deyab, *Mater. Chem. Phys.*, 89 (2005) 183.
29. A.Y. Musa, W. Ahmoda, A.A. Al-Amiery, A.A.H. Kadhum, A.B. Mohamad, *J. Struct. Chem.*, 54 (2013) 301.

30. I.B. Obot, N.O. Obi-Egbedi, E.E. Ebenso, A.S. Afolabi, E. E Oguzie, *Res. Chem. Intermed.*, 39 (2012) 1927.
31. I. Lukovits, E. Kalman, F. Zucchi, *Corrosion*, 57 (2001) 3.
32. S.Q. Hu, A.L. Guo, Y.G. Yan, X.L. Jia, Y.F. Geng, W.Y. Guo, *Comput. Theor. Chem.*, 964 (2011) 176.